



An analysis of the 2023 summer and fall marine heat waves on the Newfoundland and Labrador Shelf: the impact of stratification, winds, and advection

Nancy Soontiens¹, Heather J. Andres¹, Jonathan Coyne¹, Frédéric Cyr¹, Peter S. Galbraith², Jared Penney¹

¹Northwest Atlantic Fisheries Centre, Fisheries and Oceans Canada, St. John's, NL, A1C 5X1, Canada

²Institut Maurice-Lamontagne, Fisheries and Oceans Canada, Mont-Joli, QC, G5H 3Z4, Canada

Correspondence to: Nancy Soontiens (nancy.soontiens@dfo-mpo.gc.ca)

Abstract

In this study, we investigated a series of moderate to severe surface marine heat waves (MHWs) impacting the Newfoundland and Labrador Shelf during the summer and fall of 2023. Using a combination of ocean model reanalysis data, in situ data collected under the Atlantic Zone Monitoring Program (AZMP), and atmospheric reanalysis data, we explored several factors that contributed to the intensity of these MHWs. We concluded that first, due to an unusually cold spring and abnormally fresh conditions advected from upstream, the water column was highly stratified. Second, atmospheric conditions were calm, and wind speeds were unusually low for prolonged periods in the summer. The combination of increased stratification and lower wind speeds caused a reduction in vertical mixing, limiting the exchange of warm surface waters with colder waters below and amplifying the retention of heat near the surface. However, by the late fall, the signature of the surface heat wave had vanished when the cooler subsurface waters were mixed vertically due to increased winds, storms, and surface cooling. During the most intense MHW in July 2023, we found that this event was confined to the surface as demonstrated by temperature anomalies along several standard transects which showed a thin layer of warm anomalies in the upper 10 m and cold anomalies below. Consequently, the vertical extent and distribution of MHWs are important considerations when exploring ecosystem impacts because not all elements of the ecosystem are equally sensitive to surface conditions. Finally, these results suggest that ocean model nowcast and reanalysis products can complement observational methods for studying MHWs in near-real time over large geographic areas and at multiple depths.



24 Copyright statement

25 The works published in this journal are distributed under the Creative Commons Attribution 4.0 Licence. This licence does
26 not affect the Crown copyright work, which is re-usable under the Open Government Licence (OGL). The Creative Commons
27 Attribution 4.0 License and the OGL are interoperable and do not conflict with, reduce or limit each other.

28 © His Majesty the King in Right of Canada, 2024

29 1 Introduction

30 In the summer of 2023, the North Atlantic Ocean experienced a series of significant marine heat waves (MHWs) sparking
31 media attention and public interest in the associated record-setting high ocean temperatures. These MHWs were first detected
32 in the Northeast Atlantic in June and, later, in the Northwest Atlantic in July (Copernicus, 2023). Ocean warming and MHWs
33 can have significant impacts on the marine ecosystem (e.g., LeGrix et al., 2021; Geoffroy et al., 2023, Smith et al., 2023), air-
34 sea exchange (e.g. Edwing et al., 2024) and weather (e.g., Frölicher et al., 2018). Globally, MHWs are occurring more
35 frequently and with greater duration (Oliver et al, 2018; IPCC, 2019; IPCC, 2023). As such, it is critical to develop a more
36 complete understanding of their drivers (Oliver et al., 2021) which will lead to improved real-time monitoring efforts and
37 forecasting capabilities (e.g., McAdam et al., 2023).

38
39 Studies of MHWs in the Northwest Atlantic have documented the role of air-sea fluxes and oceanic processes like advection
40 in the onset and decay of MHWs. Schlegel et al. (2021) used statistical methods to link latent heat flux and mixed layer depth
41 as drivers of MHWs over the Northwest Atlantic continental shelf. They show that the onset of many surface MHWs in this
42 area is linked with a positive air-sea heat flux anomaly into the ocean, most often driven by latent heat flux and shortwave
43 radiation, but that the decay is more likely associated with oceanic processes like advection and mixing. Other studies have
44 correlated MHWs with large-scale atmospheric conditions and spatial variability in heat flux anomalies. For example, Perez
45 et al. (2021) link the 2015/16 MHW in the Northwest Atlantic to the position of the jet stream modifying the spatial distribution
46 of heat fluxes, a finding confirmed by Sims et al. (2022), who further correlate sea surface temperature (SST) and sea surface
47 salinity anomalies near the shelf break in a subregion (48–70° W, 40–48° N) with the North Atlantic Oscillation (NAO). These
48 studies indicate that a combination of oceanic and atmospheric processes drove the 2015/16 MHW.

49
50 In this study, we describe a series of MHWs that occurred on the Newfoundland and Labrador (NL) Shelf during the summer
51 and fall of 2023. The NL Shelf is a region of economic, environmental, and cultural importance as it supports numerous
52 commercial, recreational, and Indigenous fisheries (Templeman, 2010). The oceanographic conditions are characteristic of
53 Arctic and subarctic environments, and are influenced by the Labrador Current, which transports relatively cold and fresh
54 water equatorward along the continental shelf (e.g., Lazier and Wright, 1993; Fratantoni and Pickart, 2007). The region
55 undergoes interannual variability cycling through warm and cold phases associated with changes in air temperature, sea ice



conditions, and climate indices such as the NAO (Cyr and Galbraith, 2021). These warm and cold phases are linked to marine ecosystem characteristics such as the timing of the spring phytoplankton bloom, and primary and secondary productivity (Cyr et al., 2024a; Cyr et al., 2024b). We conduct our analysis over several geographic subregions of the NL Shelf with distinct ecosystem characteristics, as described in Section 2.2 and explore the influence of several meteorological and oceanographic phenomena such as winds, stratification, and advection on this series of MHWs. Studying the factors driving MHWs on the NL Shelf will support understanding in how these events may impact the local marine ecosystem.

2 Methods

2.1 Datasets

A number of datasets were used in this study. MHWs were characterised using the sea surface temperature (SST) from product ref. no. 1 (Table 1) which is a 1/12 degree global ocean reanalysis covering December 31, 1992 to December 25, 2023. Daily mean temperature and salinity fields were also used to describe oceanographic conditions such as stratification, depth-averaged temperature, and freshwater density. Sea ice concentration was also analysed in 2023 to characterise the monthly maximum sea ice extent defined as regions where the concentration is greater than 0.15. Following recommendations by McDougall et al. (2021), we interpreted the reanalysis prognostic temperature and salinity variables to be conservative temperature and preformed salinity – a salinity variable not affected by biogeochemistry – scaled by a factor of $u_{ps} = 35.16504/35 \text{ g kg}^{-1}$.

The reanalysis dataset was complemented by temperature and salinity profiles from product ref. no. 2 (CASTS; Table 1) which is composed of historical profiles in Atlantic Canada and the Eastern Arctic dating back to 1912, but here limited to the period 1993-2023. Many of the CASTS profiles used in this study were collected under the Atlantic Zone Monitoring Program (AZMP; Therriault et al., 1998) which routinely monitors core stations and transects at annual and seasonal frequencies. Two AZMP transects (Seal Island and Flemish Cap) and one high frequency station (Station 27) were considered in this study (Fig. 1). To facilitate comparison with the reanalysis, the CASTS potential temperature and practical salinity variables were converted to conservative temperature and preformed salinity using the Python implementation of the Gibbs-Seawater (GSW) Oceanographic Toolbox (McDougall and Barker, 2011).

Finally, 10 m wind speeds were taken from product ref. no. 3 which is a global atmospheric reanalysis (ERA5; Table 1). Daily mean wind speeds from 2023 were smoothed using an 11-day rolling mean in order to isolate synoptic-scale events by removing high-frequency variability. The 11-day window was chosen to align with the MHW calculations and is consistent with synoptic timescales of days to weeks.



85

Product Ref. No.	Product ID & type	Data Access	Documentation
1	GLOBAL_MULTIYEAR_PHY_001_030 (GLORYS12V1), numerical models	EU Copernicus Marine Service Product (2023)	Product User Manual (PUM): Dréville et al., 2023a Quality Information Document (QUID): Dréville et al., 2023b Journal article: Lellouche et al., 2021
2	CASTS, observed temperature and salinity profiles	Federated Research Data Repository, https://doi.org/10.20383/102.0739	Coyne et al., 2023
3	ERA5, atmospheric reanalyses	Copernicus Climate Change Service (2023)	Product reference: Hersbach et al., 2023 Journal article: Hersbach et al., 2020

86 **Table 1: Product reference table**

87 **2.2 Marine heat wave definitions**

88 Following Hobday et al. (2016), we defined a MHW as a period of 5 days or longer during which the daily averaged SST
 89 exceeds the climatological 90th percentile (T_{90}) for the given time of year. The World Meteorological Organization
 90 recommends, when possible, to use a 30-year time series (1991-2020) to calculate climatologies (World Meteorological
 91 Organization, 2017). In this study, because product ref. no. 1 starts in 1993, the climatology was calculated for each day of the
 92 year over 1993 to 2022. The climatological mean and 90th and 10th percentiles were determined using an 11-day window (see
 93 Hobday et al. (2016) for details) and the percentiles were smoothed using a 31-day rolling mean.

94
 95 Spatially, the analysis was performed over 1) every grid cell in the reanalysis from 65° W to 39° W and 41° N to 62° N and 2)
 96 the spatially averaged SST in regions relevant to the NL Shelf ecosystem. Shown in Fig. 1 (a), these regions are the Labrador
 97 Shelf (LS), the Northeast Newfoundland Shelf (NNS), the Grand Banks (GB), and Flemish Cap (FC). Each represents an area
 98 of distinct primary productivity and a well-defined food web system (Open Government, 2014; Pepin et al., 2014). A fifth
 99 region covering the entire NL Shelf (Fig. 1 (b)) was also included.

100
 101 Finally, we followed Hobday et al. (2018) to define four heat wave categories as follows: moderate ($T_{90} \leq T < T_{90} + \Delta$),
 102 strong ($T_{90} + \Delta \leq T < T_{90} + 2\Delta$), severe ($T_{90} + 2\Delta \leq T < T_{90} + 3\Delta$), and extreme ($T \geq T_{90} + 3\Delta$) where T is the
 103 temperature, and Δ is the difference between T_{90} and the climatological mean. Some additional MHW metrics, including the



start and end dates, duration, and mean, maximum, and cumulative intensities, suggested by Hobday et al. (2016) are reported in Table 2.

2.3 Stratification, depth-averaged temperature, and freshwater density

The 2023 daily time series and climatologies (1993-2022) of three additional metrics (stratification, depth-averaged temperature, and freshwater density) were calculated. The metric climatologies were determined using the same methodology as applied to the SST climatologies. First, the stratification was assessed by the vertical maximum of the squared-buoyancy frequency (N^2) calculated over the entire water column using the GSW Oceanographic Toolbox (McDougall and Barker, 2011). A large value indicates strong stratification which can limit the vertical exchange of heat and salt content. This quantity was analysed as a spatial average over each region and at the grid cell closest to Station 27. Second, the depth-averaged temperature and freshwater density were used to examine the daily time evolution of temperature and freshwater content in the uppermost 20 metres spatially averaged over the NL Shelf region. The depth-averaged temperature is defined as

$$T_{z_1-z_2} = \frac{\int_{z_1}^{z_2} T dz}{\int_{z_1}^{z_2} dz},$$

where T is the temperature, z_1 and z_2 are the depth levels over which the integral is calculated. The freshwater density is

$$FWD_{z_1-z_2} = \frac{\int_{z_1}^{z_2} \frac{\rho(T,S,p) S_{ref} - S}{\rho(T,0,p) S_{ref}} dz}{\int_{z_1}^{z_2} dz},$$

where $\rho(T,S,p)$ is the in situ density calculated with the GSW Oceanographic Toolbox, S is the salinity, p is the pressure, $\rho(T,0,p)$ is the density of seawater with zero salinity, and S_{ref} is a reference salinity of 35 g kg⁻¹. Quantities that were spatially averaged over a region or across a transect are denoted by an overbar symbol. For example, the spatially averaged sea surface temperature over a region is defined by

$$\overline{SST} = \frac{\int_{area} SST dA}{\int_{area} dA}.$$

3 Results

From July through October, MHWs were detected over most of the Northwest Atlantic (Fig. 1). Over the NL Shelf, MHW categories mainly ranged from moderate to severe with spatial variability in the intensity and duration. No MHWs were present continuously throughout the entire July to October period, but rather a series of MHWs transpired in each region (Table 2). Each MHW period was associated with higher-than-typical stratification, in many cases exceeding the 90th percentile. The most intense and longest duration MHW began in July in FC. Each of the other subregions experienced their strongest MHW (in terms of maximum and mean intensity) around the same time, also commencing in July. A large portion of the southern GB received relatively short duration and low intensity MHWs while both LS and NNS contained localised areas of higher



intensity MHWs (e.g., up to severe) that were approximately colocated with areas of greater total MHW days in the July through October period (Fig. 1).

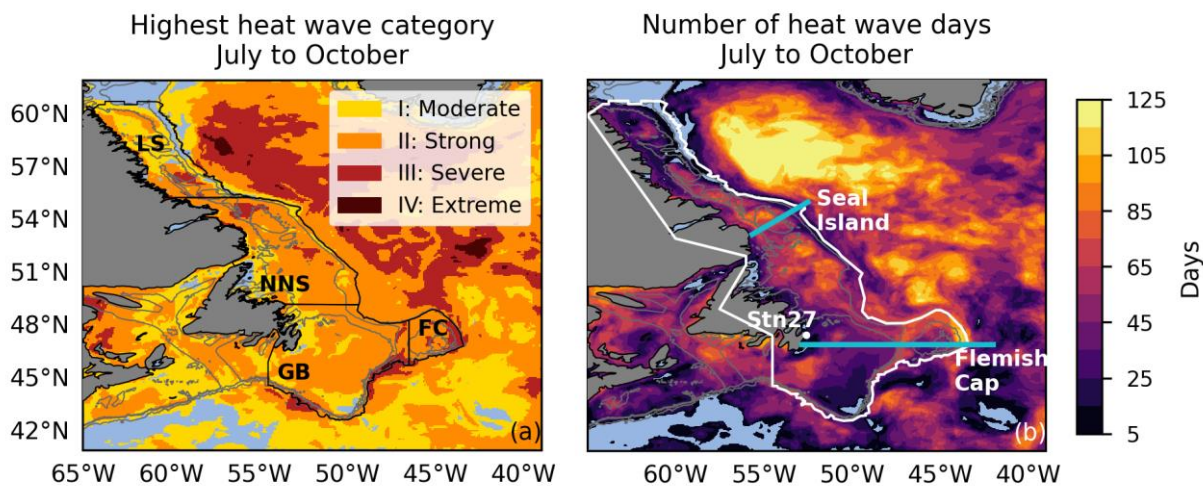


Figure 1: (a) Spatial map of highest heat wave categories in July through October 2023 calculated from the ocean reanalysis (product ref. no. 1). The thin black lines represent the regions over which MHW statistics are calculated: Labrador Shelf (LS), Northeast Newfoundland Shelf (NNS), Grand Banks (GB), and Flemish Cap (FC). (b) Total number of heat wave days July through October 2023 (maximum 122 days). The white line represents the polygon used to define the entire NL Shelf. Standard AZMP transects Seal Island and Flemish Cap are represented by the blue lines. The white dot is the location of Station 27 (Stn27). On both plots, grey lines are the 200 m, 500 m, and 1500 m bathymetry contours. The polygons defining the subregions contain information licensed under the Open Government Canada Licence - Canada.

When the MHW metrics were determined by spatially averaging over the entire NL Shelf, the result was three MHW periods (Table 2). These three periods approximately coincide with the MHW periods identified in the regional analysis. However, the late August MHW in FC and NNS is not captured in the larger spatial average. Nevertheless, we used MHW metrics over the entire NL Shelf region to identify local oceanographic and meteorological conditions that contributed to the evolution of this series of MHWs.



149

Region	t_s	t_e	D (days)	i_{max} (°C)	i_{mean} (°C)	i_{cum} (°C days)	$\langle \overline{N^2} \rangle$ (10^{-4} s^{-2})	$\langle \overline{N_{clim}^2} \rangle$ (10^{-4} s^{-2})	$\langle \overline{N_{90th}^2} \rangle$ (10^{-4} s^{-2})
Labrador Shelf (LS)	2023-07-16	2023-07-27	11	1.98	1.71	206.46	12.94	10.35	12.7
	2023-10-07	2023-10-23	16	1.05	0.91	233.36	5.5	4.23	6.0
Northeast Newfoundland Shelf (NNS)	2023-07-16	2023-08-10	25	3.13	2.42	1513.31	14.48	9.09	10.7
	2023-08-22	2023-09-01	10	2.08	1.86	186.08	13.54	9.85	11.52
	2023-09-14	2023-09-19	5	1.63	1.52	38.12	10.25	7.17	9.06
	2023-10-08	2023-10-30	22	1.68	1.28	564.96	5.61	4.17	5.84
Grand Banks (GB)	2023-07-15	2023-08-06	22	3.99	2.84	1373.86	12.97	7.5	9.07
	2023-09-07	2023-09-24	17	2.94	2.14	618.02	12.17	9.67	10.94
Flemish Cap (FC)	2023-07-08	2023-08-08	31	5.52	3.69	3542.3	9.83	4.88	6.46
	2023-08-27	2023-09-01	5	1.98	1.75	43.72	9.4	7.47	9.11
	2023-09-05	2023-09-24	19	3.48	2.69	971.81	10.51	7.91	9.35
Entire NL Shelf	2023-07-14	2023-08-08	25	2.72	1.98	1235.43	11.75	10.27	12.65
	2023-09-06	2023-09-23	17	1.74	1.33	385.09	7.78	6.2	8.93
	2023-10-10	2023-10-24	14	1.27	1.02	200.84	5.35	4.17	5.87

Table 2: MHW metrics and stratification for each region and the entire NL Shelf calculated from the ocean reanalysis (product ref. no. 1). For MHW metrics, t_s and t_e are the start and end dates of each heat wave, D is the duration, i_{max} , i_{mean} , and i_{cum} are the maximum, mean, and cumulative intensities derived from the spatially averaged sea surface temperature anomaly during each heat wave period. For stratification, $\overline{N^2}$, $\overline{N_{clim}^2}$, $\overline{N_{90th}^2}$ are the spatially averaged quantities from 2023, the 1993-2022 climatological mean, and the 1993-2022 90th percentile, respectively. The angled brackets, $\langle \rangle$, denote a time average over the MHW period.

An intriguing feature of this series of MHWs was that it was pre-conditioned by an unusually cold spring (Fig. 2 (a)-(b)). In mid-June, spatially averaged SST anomalies over the entire shelf were as low as -0.56°C . In some areas, such as the southwestern extent of GB and coastal regions of southern NNS, monthly averaged SST anomalies in June were below -1.50°C (Fig. 2 (b)). In contrast, anomalies in July were positive over nearly the entire NL Shelf and the highest anomalies occurred in the FC region. High positive anomalies continued over most of the NL Shelf in August, but the highest anomalies shifted to the NNS region. In September, high anomalies returned to the FC area and were concentrated in areas with steep bathymetric gradients that are strongly influenced by the Labrador Current, suggesting a possible advective source of warm water from upstream. Finally, October saw a reduction in the strength of the anomalies, but SSTs were still warmer than usual across the entire NL Shelf.

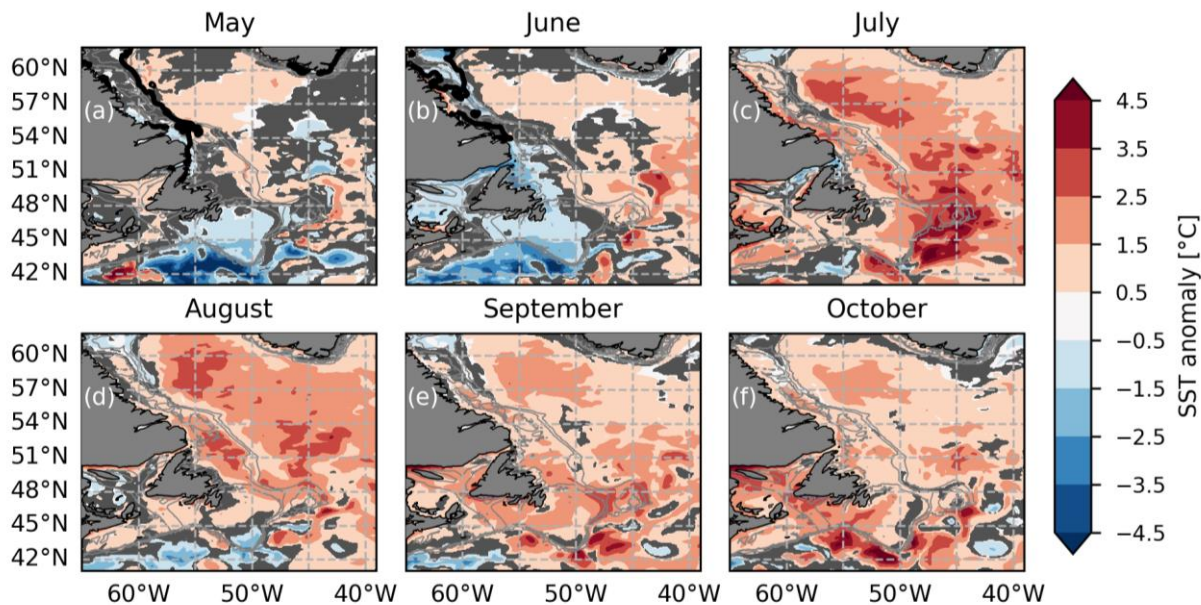


Figure 2: Sea surface temperature anomaly from the ocean reanalysis (product ref. no. 1) averaged over (a) May, (b) June, (c) July, (d) August, (e) September, and (f) October 2023. A reference period of 1993-2022 is used to calculate climatology. Thin grey lines are the 200 m, 500 m, and 1500 m bathymetry contours. The thick black contours in (a) and (b) indicate the monthly maximum sea ice extent from the ocean reanalysis in 2023. The ocean reanalysis had no sea ice in this area from July through October. The grey shading represents regions where the absolute value of the anomaly is less than 0.5 times the interannual standard deviation of the monthly mean sea surface temperature.

In addition to unusually cold spring SSTs, subsurface temperatures from about 10-50 m in July were below normal across the Seal Island and Flemish Cap transects in both reanalysis and AZMP profiles (Fig. 3 (a)-(b)). Both transects displayed a very warm surface layer reaching to approximately 10 m in depth, in contrast to the signal at depth. Additionally, the Seal Island transect showed anomalously fresh conditions in the upper 20 m across most of the transect in July (Fig. 3 (c)), particularly over the shelf break. Along the Flemish Cap transect, fresh signals were not as strong as at Seal Island at this time, but salinity anomalies between -0.25 g kg^{-1} and -0.75 g kg^{-1} were apparent near the coast.

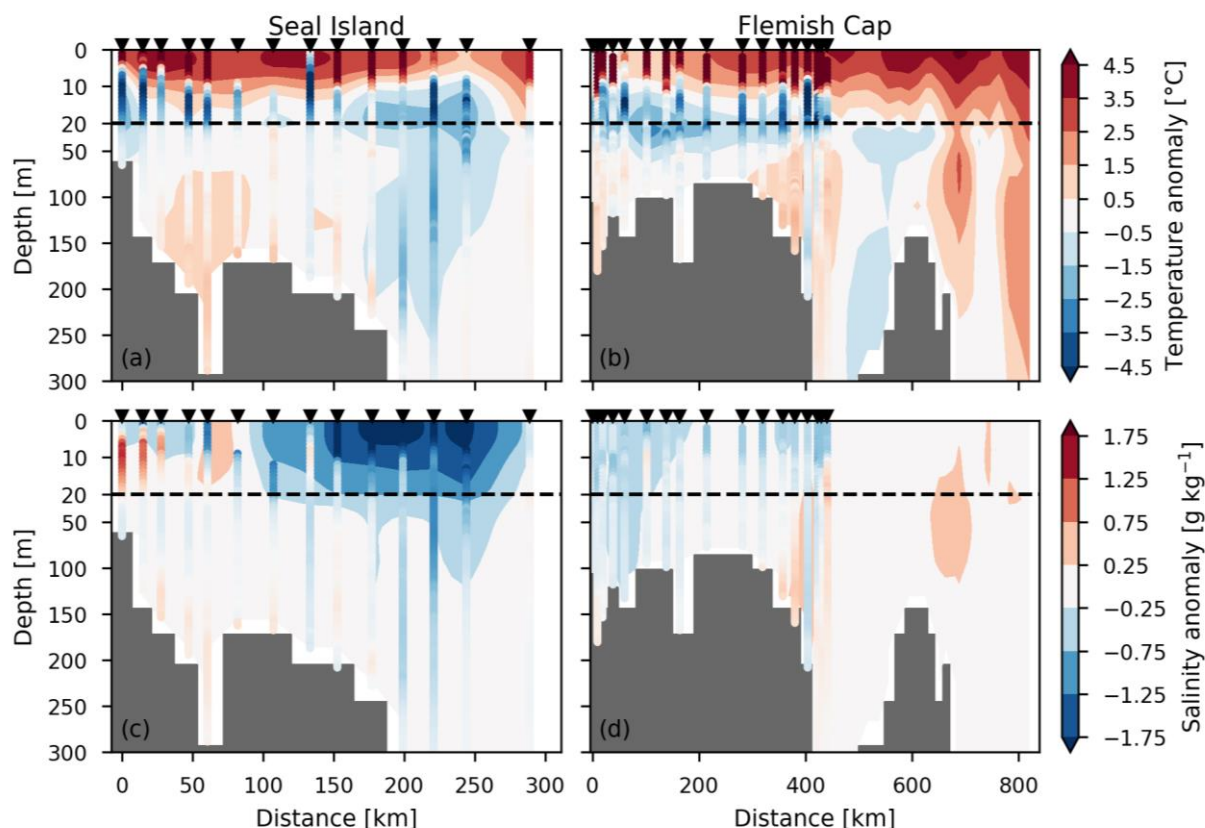


Figure 3: Temperature (top) and salinity (bottom) anomalies along the Seal Island (left) and Flemish Cap (right) transects shown for AZMP July 2023 occupation dates. For Seal Island, the AZMP occupation occurred on July 25. For Flemish Cap, the stations inshore of 200 km were sampled on July 20 and the remaining were sampled on July 30. Ocean reanalysis anomalies (product ref. no. 1) are shown in shaded contours, and AZMP anomalies (product ref. no. 2) are shown in the coloured circles which appear as lines extending from top to bottom. A reference period of 1993–2022 is used to calculate climatologies for both the reanalysis and AZMP. For AZMP, all July and August occupations in the reference period were used to construct the climatology. The black triangles represent the positions of the AZMP stations sampled in 2023. Note the difference in vertical scale above and below 20 m (black dashed line).

The anomaly structures of vertical profiles for both temperature and salinity suggest high stratification during the AZMP occupations in July. Indeed, high stratification was apparent at Station 27 in both the reanalysis and AZMP data throughout nearly the entire summer and early fall (Fig. 4 (b)). High stratification is partially explained by the anomalously cold spring which resulted in a colder than typical subsurface layer and, in turn, strong vertical temperature gradients when surface warming commenced as a result of solar heating. Furthermore, the 0–20 m freshwater density in Fig. 4 (e) reveals fresher than typical near-surface conditions from July through October. This fresh anomaly was concentrated in the upper 20 m (see Fig. A1), further explaining the higher than usual stratification. The source of the fresh anomaly is not yet clear but it is present in both the reanalysis and observations (Fig. 3 (c) and (d)).



197 Another factor that impacts stratification is the degree of vertical mixing introduced by wind forcing at the ocean surface. The
198 10 m wind speeds from ERA5 at Station 27 shown in Fig. 4 (c) demonstrate that periods of below average wind speeds in the
199 summer and fall (e.g., early July, mid August to early September, and late September to early October) preceded the three heat
200 wave periods identified in Fig. 4. Furthermore, a return to average wind speeds preceded the end of each heat wave period
201 with the exception of a wind event in mid-July. Granted, this mid-July event corresponded with a reduction in the Station 27
202 stratification and was followed by a slight dip in the spatially averaged SST as the cold subsurface layer was mixed with the
203 warm surface. Although the periods of average wind speeds were linked with a pause in heat wave conditions, it is likely that
204 these wind events were not strong enough to significantly erode the strongly stratified conditions introduced by a cold spring
205 and fresh early summer. In turn, cold subsurface conditions (from about 20-50 m; not shown), high stratification, and retention
206 of heat near the surface persisted throughout most of the summer and fall.

207

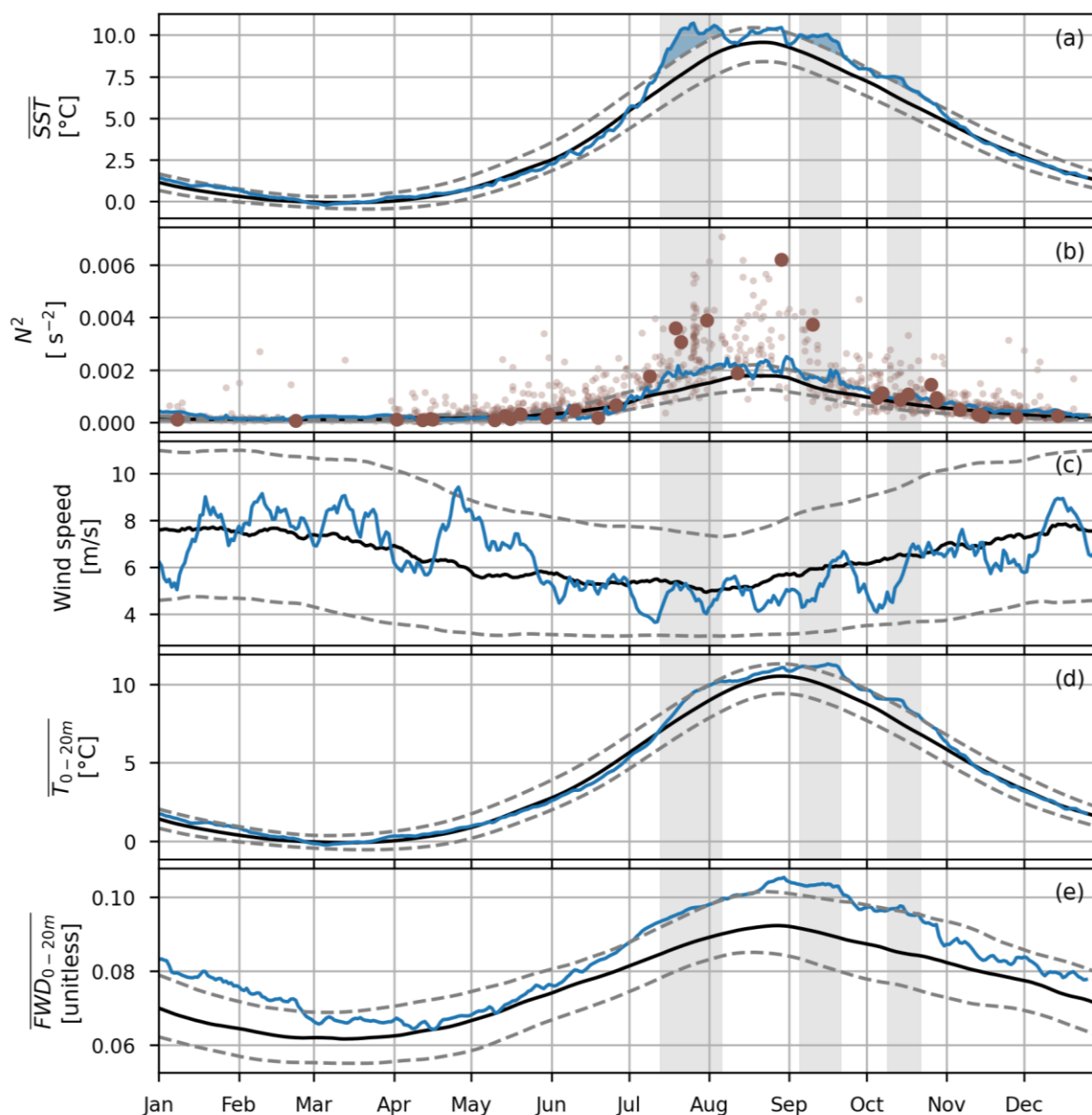


Figure 4: (a) Time series of ocean reanalysis (product ref. no. 1) sea surface temperature averaged over the NL Shelf for 2023 (blue), the 1993-2022 climatology (black), and the 1993-2022 10th and 90th percentile (grey dashed). Heat wave periods are indicated by the grey shading. (b) As in (a) but for the maximum squared buoyancy frequency at Station 27. Large dark brown dots represent observations from AZMP (product ref. no. 2) during 2023 while small light brown dots represent all observations (product ref. no. 2) in the 1993-2022 reference period. (c) As in (a) but for the ERA5 10 metre wind speed (product ref. no. 3) at Station 27. (d) As in (a) but for the ocean reanalysis (product ref. no. 1) depth-averaged temperature from 0-20 m spatially averaged over the NL Shelf. (e) As in (d) but for freshwater density from 0-20m.



4 Discussion and conclusions

4.1 Factors contributing to the 2023 MHWs

A combination of factors illustrated Fig. 5 resulted in the series of MHWs detected on the NL Shelf in 2023. First, stratification increased as the surface layer warmed in July. In addition, conditions were fresher than typical in the upper 20 m (e.g. Fig. 3 (c), Fig. 4 (e), Fig. A1 (c)-(d)). Although the source of these fresh conditions was not analysed in this work, other studies link abrupt sea ice melt and strong stratification with intensified surface MHWs in the Arctic (see e.g. Barkhordarian et al., 2024; Richaud et al., 2024). In 2023, sea ice conditions on the Labrador Shelf were above normal in June leading to late last occurrence on the southern Labrador Shelf (Galbraith et al., 2024). Finally, periods of low winds maintained that stratification by limiting vertical mixing. As a result, heat was retained near the surface resulting in a series of MHWs throughout the summer and fall. This series was interrupted by occasional wind events which excited vertical mixing and reduced SSTs.

The role of advection should also be considered. The Labrador Current is responsible for transporting water properties southward along the NL Shelf. For example, the anomalously fresh conditions detected at Seal Island in July (Fig. 3 (c)) were transported south carrying with them properties such as high stratification. Indeed, Fig. 2 (d)-(f) shows signs that warm anomalies were potentially associated with transport from NNS in August to the outer (inner) edges of GB (FC) in September. A bifurcation of the Labrador Current exists near the northern boundary of GB, possibly directing some of the conditions associated with warm anomalies along the coast of GB in October. However, the October onset of MWHs in LS and NNS cannot be explained by transport and is more likely linked with local meteorological and oceanographic conditions. A more thorough investigation quantifying the magnitude of these factors is considered for future work.

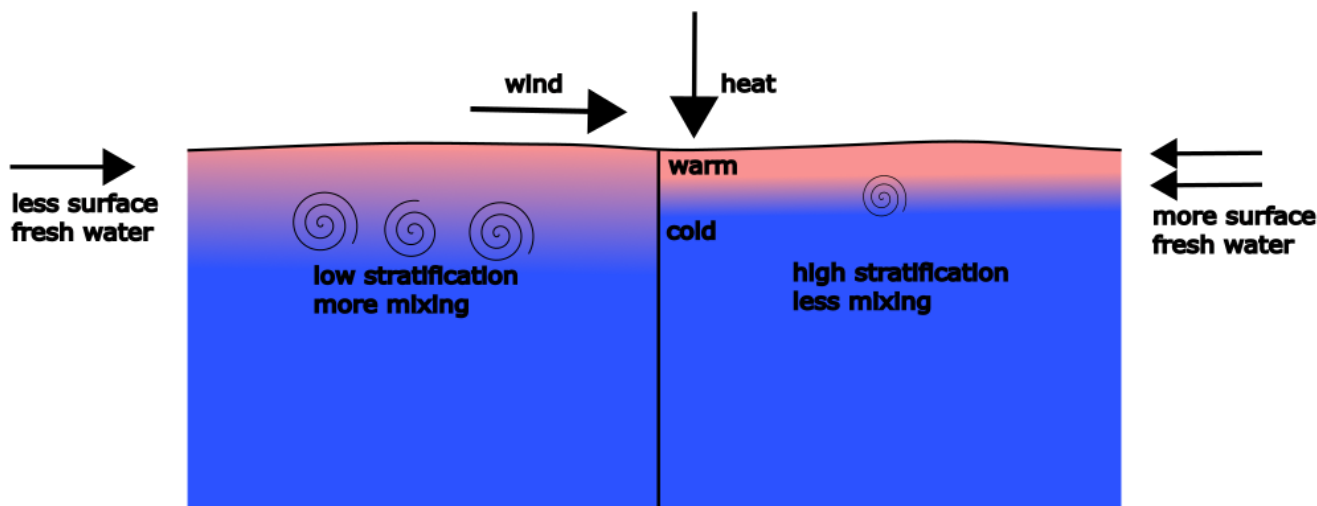


Figure 5: Schematic diagram describing the role of increased stratification on surface MHWs. On the left, less surface fresh water leads to lower stratification and more mixing. On the right, more surface fresh water leads to higher stratification and less mixing. Both scenarios receive the same heat flux and wind forcing at the surface. The case with more surface fresh water results in higher SSTs because the heat is confined to the surface due to high stratification.

4.2 Sensitivity to climatological period

We explored the sensitivity of the MHW metrics to the climatological period by considering climatologies over 1993-2019 and 1996-2022. These two periods were selected to control for the relatively warm conditions from 2020-2022 and cold conditions from 1993-1995 (Galbraith et al., 2024). We found that, relative to the 1993-2022 climatology, the duration of a regional MHW event could be modified by up to four days. More typically, the duration was modified by a day or two. In addition, the maximum intensity was no more than 0.19 °C different when compared to the original 1993-2022 climatological period. The largest impact occurred during the October MHW over the entire NL Shelf which was shortened by seven days when using the 1996-2022 period and lengthened by six days when using the 1993-2019 period. Furthermore, when using the 1993-2019 climatology, the temperature increase in late August shown in Fig. 4 (a) achieved the MHW definition on the NL Shelf and the FC and GB regions both achieved MHWs in October. Finally, the two 5-day long MHWs in FC and NNS were not long enough to meet the MHW definition when using the 1996-2022 climatology. Overall, our interpretations of the factors contributing to MHWs were not impacted by modifying the climatological period.

4.3 Connection to the ecosystem

The timing of the spring bloom on the NL Shelf is linked with oceanographic conditions such as stratification and temperature, with earlier blooms occurring during warmer climate conditions and associated with earlier onset of stratification (Wu et al.,

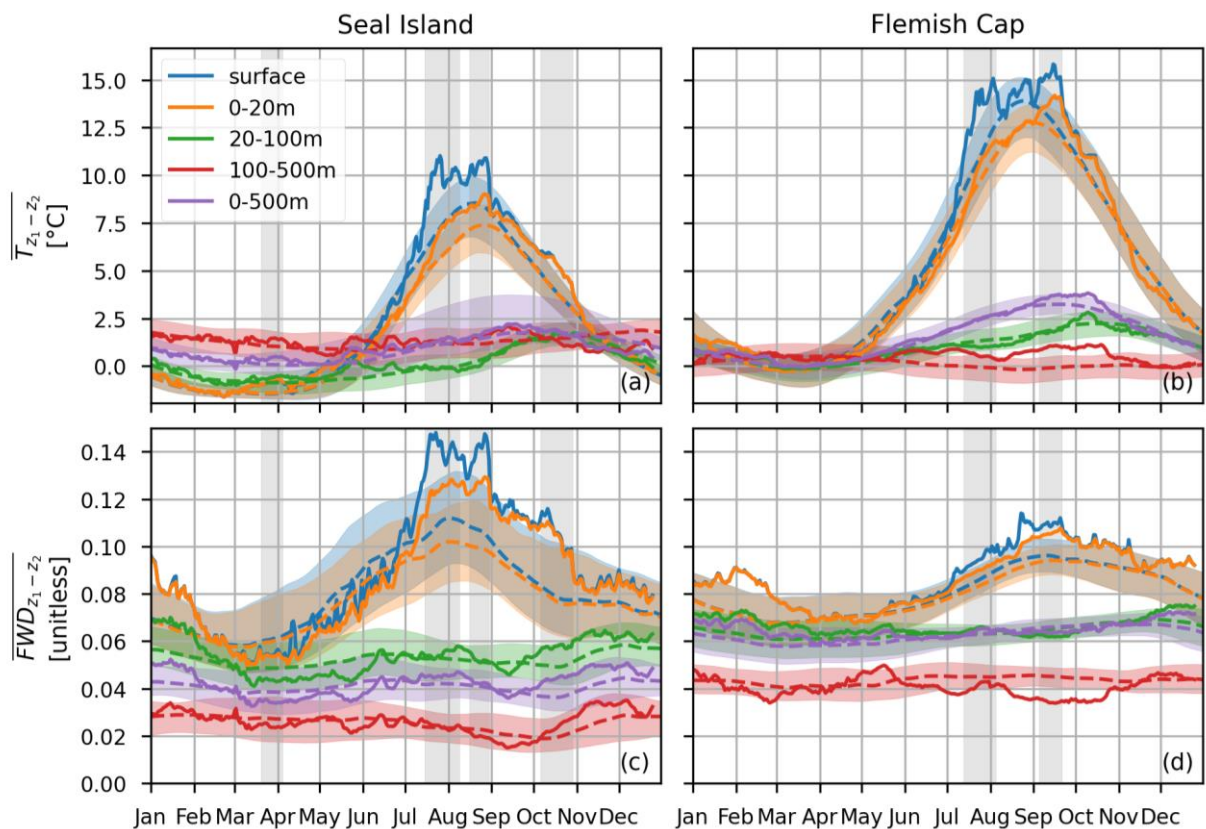


2007; Zhao et al., 2013; Cyr et al., 2024a). Despite the unusually cold SST during the spring (Fig. 2 (a) and (b)), the timing of the spring bloom was near-normal in GB and NNS in 2023 (Galbraith et al., 2024). Interestingly, spring bloom intensity in NNS was higher than normal and the fall bloom occurred earlier and was more intense than usual, potentially promoted by warmer surface waters in August or high nutrient inventories. Furthermore, the strong stratification throughout the summer and fall (Fig. 4 (b), Table 2) might also have contributed to the later timing of the fall bloom in GB and FC by limiting the transport of nutrients to surface waters. Overall, the impact of the 2023 MHWs on primary productivity in this region is not yet clear and deserves further exploration.

Besides impacts on primary productivity, MHWs can potentially influence higher trophic levels and marine habitats on the NL Shelf. For example, Dempson et al. (2016) noted warm climate conditions are linked with earlier river return times for Atlantic salmon migrating in this region. Yet, despite the warm SST in the summer and fall of 2023, the unusually cold spring could also impact salmon migration pathways and return timing. Ocean climate can also influence the spawning timing of capelin, a key pelagic species on the NL Shelf, with warmer than normal conditions associated with earlier spawning times (Murphy et al., 2021). Overall, on the NL Shelf, SSTs have shown considerable warming trends in recent years, with the last 3 years establishing new warm records during the ice-free period, respectively in 2021, 2023, and 2022 in increasing order (Galbraith et al., 2024). Surface MHWs were also detected on the NL Shelf in 2020-2022 indicating a need for more research into how these events impact the ecosystem. One area of interest is the vertical distribution of MHWs because not all elements of the marine ecosystem are impacted by high sea surface temperatures. Furthermore, regional differences in MHW intensity, frequency, and duration are important elements when considering ecosystem impacts. Tools such as ocean model reanalyses, analyses, and forecasts can aid in near real-time monitoring by linking surface MHWs with vertical characteristics such as stratification and by exploring spatial structure in remote areas that are difficult to study directly with observations.



278 **Appendix**



279
280 **Figure A1: Depth-averaged temperature (top) and freshwater density (bottom) from the ocean reanalysis (product ref. no. 1)**
281 **averaged across the Seal Island (left) and Flemish Cap transects (right). Results are shown out to the 500 m isobath for the surface**
282 **(blue), 0-20m (orange), 20-100m (green), 100-500m (red), and 0-500m (purple). The solid line is the 2023 time series, the dashed line**
283 **is the 1993-2022 climatology, and the shaded areas represent the 10th and 90th percentiles from the 1993-2022 period. Grey shaded**
284 **rectangles represent heat wave periods based on SST along each transect.**

285 **Data and code availability**

286 The data used in this study are available as described in Table 1. The code used in this study can be accessed via a GitLab
287 repository upon request via email to the corresponding author.

288 **Author contribution**

289 NS conducted the analysis, produced the visualisations, and prepared the initial manuscript draft. NS, HJA, and JC organised
290 and curated data. All authors contributed to conceptualization of the study, discussions on methodology and results, and editing
291 and reviewing the manuscript.



292 **Competing interests**

293 The authors declare that they have no conflict of interest.

294 **Acknowledgements**

295 Hersbach et al. (2023) was downloaded from the Copernicus Climate Change Service (2023). The results for ERA5 contain
 296 modified Copernicus Climate Change Service information 1993-2023. Neither the European Commission nor ECMWF is
 297 responsible for any use that may be made of the Copernicus information or data it contains. We greatly appreciate input and
 298 discussions with Dr. David Bélanger regarding 2023 nutrient inventories and primary productivity and thoughtful comments
 299 from Dr. Pierre Pepin. This work is a contribution to the science mission of the Atlantic Zone Monitoring Program.

300 **References**

- 301 Barkhordarian, A., Nielsen, D.M., Olonscheck, D., and Baehr, J.: Arctic marine heatwaves forced by greenhouse gases and
 302 triggered by abrupt sea-ice melt, *Commun. Earth Environ.*, 5, 57, <https://doi.org/10.1038/s43247-024-01215-y>, 2024.
- 303
- 304 Copernicus Climate Change Service: ERA5 hourly data on single levels from 1940 to present. Copernicus Climate Change
 305 Service (C3S) Climate Data Store (CDS), DOI: 10.24381/cds.adbb2d47, last access: 04 April 2024, 2023.
- 306 Copernicus: <https://climate.copernicus.eu/global-sea-surface-temperature-reaches-record-high>, last access: 08 May 2024,
 307 2023.
- 308
- 309 Coyne, J., Cyr, F., Donnet, S., Galbraith, P., Geoffroy, M., Hebert, D., Layton, C., Ratsimandresy, A., Snook, S., Soontiens,
 310 N., and Walkusz, W.: Canadian Atlantic Shelf Temperature-Salinity (CASTS). Federated Research Data Repository [dataset],
 311 <https://doi.org/10.20383/102.0739>, 2023.
- 312
- 313 Cyr, F. and Galbraith, P. S.: A climate index for the Newfoundland and Labrador shelf, *Earth Syst. Sci. Data*, 13, 1807–1828,
 314 <https://doi.org/10.5194/essd-13-1807-2021>, 2021.
- 315
- 316 Cyr, F., Lewis, K., Bélanger, D., Regular, P., Clay, S., and Devred, E.: Physical controls and ecological implications of the
 317 timing of the spring phytoplankton bloom on the Newfoundland and Labrador shelf, *Limnol. Oceanogr. Lett.*
 318 <https://doi.org/10.1002/lol2.10347>, 2024a.
- 319



- 320 Cyr, F., Adamack, A., Bélanger, D., Koen-Alonso, M., Mullooney, D., Murphy, H., Regular, P., and Pepin, P.: Environmental
321 Control on the Productivity of a Heavily Fished Ecosystem, Research Square [preprint], [https://doi.org/10.21203/rs.3.rs-](https://doi.org/10.21203/rs.3.rs-4108948/v1)
322 [4108948/v1](https://doi.org/10.21203/rs.3.rs-4108948/v1), 27 March 2024b.
- 323
- 324 Dempson, B., Schwarz, C.J., Bradbury, I.R., Robertson, M.J., Veinott, G., Poole, R., and Colbourne, E.: Influence of climate
325 and abundance on migration timing of adult Atlantic salmon (*Salmo salar*) among rivers in Newfoundland and Labrador, *Ecol.*
326 *Freshwater Fish*, 26, 247-259, <https://doi.org/10.1111/eff.12271>, 2017.
- 327
- 328 Drévillon, M., Fernandez, E., Lellouche, J.M.: EU Copernicus Marine Service Product User Manual for the Global Ocean
329 Physics Reanalysis, GLOBAL_MULTIYEAR_PHY_001_030, Issue 1.5, Mercator Ocean International,
330 <https://catalogue.marine.copernicus.eu/documents/PUM/CMEMS-GLO-PUM-001-030.pdf>, last access: 19 March 2024, 2023
- 331
- 332 Drévillon, M., Lellouche, J.M., Régnier, C., Garric, G., Bricaud, C., Hernandez, O., and Bourdallé-Badie, R.: EU Copernicus
333 Marine Service Quality Information Document for the Global Ocean Physics Reanalysis,
334 GLOBAL_MULTIYEAR_PHY_001_030, Issue 1.6, Mercator Ocean International,
335 <https://catalogue.marine.copernicus.eu/documents/QUID/CMEMS-GLO-QUID-001-030.pdf>, last access: 19 March 2024,
336 2023
- 337
- 338 Edwing, K., Wu, Z., Lu, W., Li, X., Cai, W.-J., and Yan, X.-H.: Impact of Marine Heatwaves on Air-Sea CO₂ Flux Along the
339 US East Coast, *Geophys. Res. Lett.*, 51, e2023GL105363, <https://doi.org/10.1029/2023GL105363>, 2024.
- 340
- 341 EU Copernicus Marine Service Product: Global Ocean Physics Reanalysis, Mercator Ocean International [dataset],
342 <https://doi.org/10.48670/moi-00021>, 2023.
- 343
- 344 Fratantoni, P. S., and Pickart, R. S.: The western North Atlantic shelfbreak current system in summer, *J. Phys. Oceanogr.*,
345 37(10), 2509-2533, <https://doi.org/10.1175/JPO3123.1>, 2007.
- 346
- 347 Frölicher, T.L., Laufkötter, C.: Emerging risks from marine heat waves, *Nat. Commun.*, 9, 650,
348 <https://doi.org/10.1038/s41467-018-03163-6>, 2018.
- 349
- 350 Galbraith, P. S., Blais, M., Lizotte, M., Cyr, F., Bélanger, D., Casault, B., Clay, S., Layton, C., Starr, M., Chassé, J., Azetsu-
351 Scott, K., Coyne, J., Devred, E., Gabriel, C.-E., Johnson, C. L., Maillet, G., Pepin, P., Plourde, S., Ringuette, M. Shaw, J.-L.,
352 Oceanographic conditions in the Atlantic zone in 2023, *Can. Tech. Rep. Hydro. and Ocean Sci.*, 379 : v + 39 p., 2024.
- 353



- 354 Geoffroy, M., Bouchard, C., Flores, H., Robert, D., Gjøsæter, H., Hoover, C., Hop, H., Hussey, N. E., Nahrgang, J., Steiner,
355 N., Bender, M., Berge, J., Castellani, G., Chernova, N., Copeman, L., David, C. L., Deary, A., Divoky, G., Dolgov, A. V.,
356 Duffy-Anderson, J., Dupont, N., Durant, J. M., Elliott, K., Gauthier, S., Goldstein, E. D., Gradinger, R., Hedges, K., Herbig,
357 J., Laurel, B., Loseto, L., Maes, S., Mark, F. C., Mosbech, A., Pedro, S., Pettitt-Wade, H., Prokopchuk, I., Renaud, P. E.,
358 Schembri, S., Vestfals, C., and Walkusz, W.: The circumpolar impacts of climate change and anthropogenic stressors on Arctic
359 cod (*Boreogadus saida*) and its ecosystem, *Elem. Sci. Anth.*, 11, 1, <https://doi.org/10.1525/elementa.2022.00097>, 2023.
- 360
- 361 Hersbach H., Bell B., Berrisford P., Hirahara, S., Horányi, A., Muñoz-Sabater, J., Nicolas, J., Peubey, C., Radu, R., Schepers,
362 D., Simmons, A., Soci, C., Abdalla, S., Abellan, X., Balsamo, G., Bechtold, P., Biavati, G., Bidlot, J., Bonavita, M., De Chiara,
363 G., Dahlgren, P., Dee, D., Diamantakis, M., Dragani, R., Flemming, J., Forbes, R., Fuentes, M., Geer, A., Haimberger, L.,
364 Healy, S., Hogan, R. J., Hólm, E., Janisková, M., Keeley, S., Laloyaux, P., Lopez, P., Lupu, C., Radnoti, G., de Rosnay, P.,
365 Rozum, I., Vamborg, F., Villaume, S., and Thépaut, J.-N.: The ERA5 global reanalysis. *Q. J. R. Meteorol. Soc.*, 146, 1999–
366 2049. <https://doi.org/10.1002/qj.3803>, 2020.
- 367
- 368 Hersbach, H., Bell, B., Berrisford, P., Biavati, G., Horányi, A., Muñoz Sabater, J., Nicolas, J., Peubey, C., Radu, R., Rozum,
369 I., Schepers, D., Simmons, A., Soci, C., Dee, D., Thépaut, J.-N: ERA5 hourly data on single levels from 1940 to present.
370 Copernicus Climate Change Service (C3S) Climate Data Store (CDS), DOI: 10.24381/cds.adbb2d47, last access: 05 April
371 2024, 2023.
- 372
- 373 Hobday, A. J., Alexander, L. V., Perkins, S. E., Smale, D. A., Straub, S. C., Oliver, E. C. J., Benthuyssen, J. A., Burrows, M.
374 T., Donat, M. G., Feng, M., Holbrook, N. J., Moore, P. J., Scannell, H. A., Sen Gupta, A., and Wernberg, T.: A hierarchical
375 approach to defining marine heatwaves, *Prog. Oceanogr.* 141, 227–238, <https://doi.org/10.1016/j.pocean.2015.12.014>, 2016.
- 376
- 377 Hobday, A. J., Oliver, E. C. J., Sen Gupta, A., Benthuyssen, J. A., Burrows, M. T., Donat, M. G., Holbrook, N. J., Moore, P.
378 J., Thomsen, M. S., Wernberg, T., Smale, D. A.: Categorizing and naming marine heatwaves, *Oceanography*, 31(2), 162–173,
379 <https://doi.org/10.5670/oceanog.2018.205>, 2018.
- 380
- 381 IPCC: IPCC Special Report on the Ocean and Cryosphere in a Changing Climate [H.-O. Pörtner, D.C. Roberts, V. Masson-
382 Delmotte, P. Zhai, M. Tignor, E. Poloczanska, K. Mintenbeck, A. Alegría, M. Nicolai, A. Okem, J. Petzold, B. Rama, N.M.
383 Weyer (eds.)]. Cambridge University Press, Cambridge, UK and New York, NY, USA, 755 pp.
384 <https://doi.org/10.1017/9781009157964>, 2019
- 385



- 386 IPCC: Climate Change 2023: Synthesis Report. Contribution of Working Groups I, II and III to the Sixth Assessment Report
387 of the Intergovernmental Panel on Climate Change [Core Writing Team, H. Lee and J. Romero (eds.)]. IPCC, Geneva,
388 Switzerland, pp. 35-115, doi: [10.59327/IPCC/AR6-9789291691647](https://doi.org/10.59327/IPCC/AR6-9789291691647), 2023.
- 389
- 390 Lazier, J. R. N., and Wright, D. G.: Annual velocity variations in the Labrador Current, J. Phys. Oceanogr., 23(4), 659-678,
391 [https://doi.org/10.1175/1520-0485\(1993\)023<0659:AVVITL>2.0.CO;2](https://doi.org/10.1175/1520-0485(1993)023<0659:AVVITL>2.0.CO;2), 1993.
- 392
- 393 Le Grix, N., Zscheischler, J., Laufkötter, C., Rousseaux, C. S., and Frölicher, T. L.: Compound high-temperature and low-
394 chlorophyll extremes in the ocean over the satellite period, Biogeosciences, 18, 2119–2137, [https://doi.org/10.5194/bg-18-](https://doi.org/10.5194/bg-18-2119-2021)
395 2119-2021, 2021.
- 396
- 397 Lellouche, J.-M., Grenier, E., Bourdallé-Badie, R., Garric, G., Melet, A., Drévillon, M., Bricaud, C., Hamon, M., Le Galloudec,
398 O., Regnier, C., Candela, T., Testut, C.-E., Gasparin, R., Ruggiero, G., Benkiran, M., Drillet, R., and Le Traon, P.-Y.: The
399 Copernicus Global 1/12° Oceanic and Sea Ice GLORYS12 Reanalysis, Front. Earth Sci. 9, 698876,
400 <https://doi.org/10.3389/feart.2021.698876>, 2021.
- 401
- 402 McAdam, R., Masina, S., and Gualdi, S.: Seasonal forecasting of subsurface marine heatwaves, Commun. Earth Environ., 4,
403 225, <https://doi.org/10.1038/s43247-023-00892-5>, 2023.
- 404
- 405 McDougall, T. J. and Barker, P. M.: Getting started with TEOS-10 and the Gibbs Seawater (GSW) Oceanographic Toolbox,
406 28 pp., SCOR/IAPSO WG127, ISBN 978-0-646-55621-5, 2011.
- 407
- 408 McDougall, T. J., Barker, P. M., Holmes, R. M., Pawlowicz, R., Griffies, S. M., and Durack, P. J.: The interpretation of
409 temperature and salinity variables in numerical ocean model output and the calculation of heat fluxes and heat content, Geosci.
410 Model Dev., 14(10), 6445-6466, <https://doi.org/10.5194/gmd-14-6445-2021>, 2021.
- 411
- 412 Murphy, M. H., Adamack, A. T. and Cyr, F.: Identifying possible drivers of the abrupt and persistent delay in capelin spawning
413 timing following the 1991 stock collapse in Newfoundland, Canada, ICES J. Mar. Sci., 78(8), 2709-2723,
414 <https://doi.org/10.1093/icesjms/fsab144>, 2021.
- 415
- 416 Oliver, E. C. J., Donat, M. G., Burrows, M.T., Moore, P. J., Smale, D. A., Alexander, L. V., Benthuyssen, J. A., Feng, M., Sen
417 Gupta, A., Hobday, A. J., Holbrook, N. J., Perkins-Kirkpatrick, S. E., Scannell, H. A., Straub, S. C., and Wernberg, T.: Longer
418 and more frequent marine heatwaves over the past century, Nat Commun., 9, 1324, [https://doi.org/10.1038/s41467-018-03732-](https://doi.org/10.1038/s41467-018-03732-9)
419 9, 2018.



- Oliver, E. C. J., Benthuisen, J. A., Darmaraki, S., Donat, M. G., Hobday, A. J., Holbrook, N. J., Schlegel, R. W., and Sen Gupta, A.: Marine heatwaves, *Annu. Rev. Mar. Sci.*, 13, 313-342, <https://doi.org/10.1146/annurev-marine-032720-095144>, 2021.
- Open Government, Ecosystem Production Units in the Northwest Atlantic, Government of Canada: <https://open.canada.ca/data/en/dataset/9a515ef8-0e2a-479e-9b25-55658eae30be>, last access: 15 February 2024, 2014.
- Pepin, P., Higdon, J., Koen-Alonso, M., Fogarty, M., and Ollerhead, N.: Application of ecoregion analysis to the identification of Ecosystem Production Units (EPUs) in the NAFO Convention Area, *NAFO Sci. Coun. Res. Doc.*, 14/069, 2014.
- Perez, E., Ryan, S., Andres, M., Gawarkiewicz, G., Ummenhofer, C. C., Bane, J., and Haines, S.: Understanding physical drivers of the 2015/16 marine heatwaves in the Northwest Atlantic, *Sci. Rep.*, 11, 17623, <https://doi.org/10.1038/s41598-021-97012-0>, 2021.
- Richaud, B., Hu, X., Darmaraki, S., Fennel, K., Lu, Y., and Oliver, E. C. J.: Drivers of marine heatwaves in the Arctic Ocean, *J. Geophys. Res-Oceans*, 129(2), e2023JC020324, <https://doi.org/10.1029/2023JC020324>, 2024
- Schlegel, R.W., Oliver, E. C. J. and Chen, K.: Drivers of Marine Heatwaves in the Northwest Atlantic: The Role of Air–Sea Interaction During Onset and Decline, *Front. Mar. Sci.*, 8, 627970, <https://doi.org/10.3389/fmars.2021.627970>, 2021.
- Sims, L. D., Subrahmanyam, B., and Trott, C. B.: Ocean–Atmosphere Variability in the Northwest Atlantic Ocean during Active Marine Heatwave Years, *Remote Sensing*, 14(12), 2913, <https://doi.org/10.3390/rs14122913>, 2022.
- Smith, K. E., Burrows, M. T., Hobday, A. J., G. King, N. G., Moore, P. J., Sen Gupta, Thomsen, M., S., Wernberg, T., and Smale, D. A.: Biological impacts of marine heatwaves, *Annu. Rev. Mar. Sci.*, 15, 119-145, <https://doi.org/10.1146/annurev-marine-032122-121437>, 2023.
- Templeman, N.D.: Ecosystem Status and Trends Report for the Newfoundland and Labrador Shelf. DFO Can. Sci. Advis. Sec. Res. Doc. 2010/026 vi + 72 pp., 2010.
- Therriault, J.-C., Petrie, B., Pepin, P., Gagnon, J., Gregory, D., Helbig, J., Herman, A., Lefaivre, D., Mitchel, M., Pelchat, B., Runge, J., and Sameoto, D.: Proposal for a Northwest Atlantic Zonal Monitoring Program, *Can. Tech. Rep. Hydro. and Ocean Sci.*, 194, vii + 57 pp., 1998.



- 454
- 455 World Meteorological Organization: WMO guidelines on the calculation of climate normals, Tech. rep., Geneva, Switzerland,
- 456 2017.
- 457
- 458 Wu, Y., Peterson, I. K., Tang, C. C. L., Platt, T., Sathyendranath, S., and Fuentes-Yaco, C.: The impact of sea ice on the
- 459 initiation of the spring bloom on the Newfoundland and Labrador Shelves, J. Plankton Res., 29(6), 509–514,
- 460 <https://doi.org/10.1093/plankt/fbm035>, 2007.
- 461
- 462 Zhao, H., Han, G., and Wang, D.: Timing and magnitude of spring bloom and effects of physical environments over the Grand
- 463 Banks of Newfoundland, J. Geophys. Res-Bioge., 118, 1385–1396, <https://doi.org/10.1002/jgrg.20102>, 2013.